ELECTRONIC SUPPLEMENTARY INFORMATION
High-Efficiency Ultrapure Green Organic Light-Emitting Diodes

Hirohiko Fukagawa[a], Taku Oono[a], Yukiko Iwasaki[a], Takuji Hatakeyama[b], Takahisa Shimizu[a]

[a]NHK Science & Technology Research Laboratories, Tokyo 1578510, Japan,
[b]Department of Chemistry, School of Science and Technology, Kwansei Gakuin University, Hyogo 6691337, Japan

*e-mail: fukagawa.h-fe@nhk.or.jp

Molecular orientation of PtN7N from XAS results;

The nitrogen K shell absorption edge of the PtN7N-doped film was measured, followed by the analysis of the molecular orientation by the extraction of the doped PtN7N component.
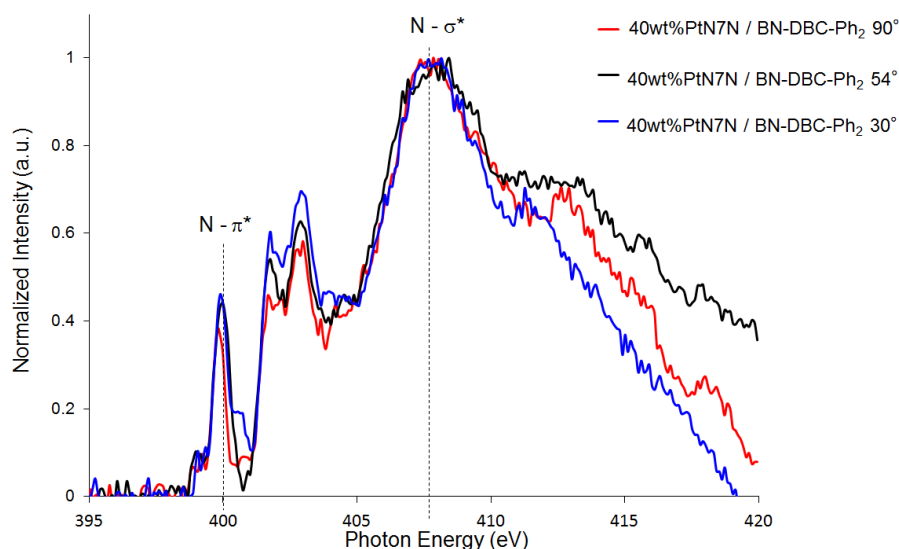
(a)
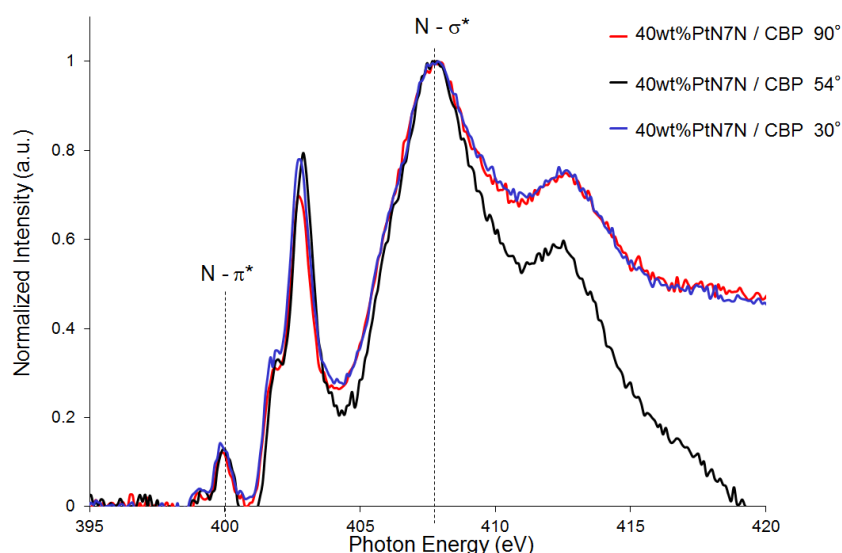
(b)

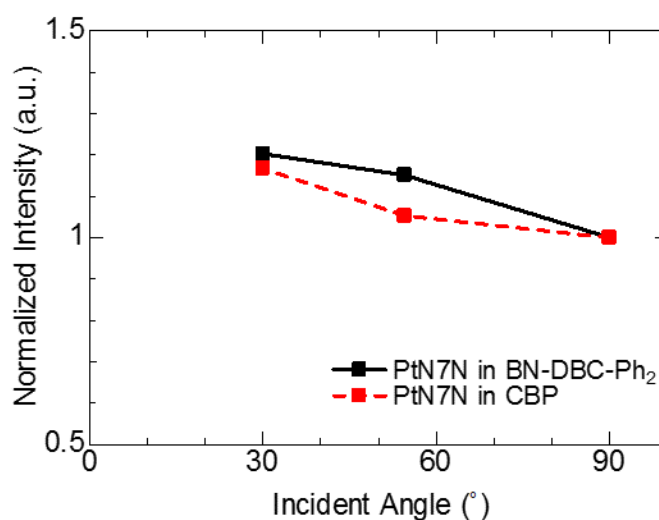**Figure S1** XAS result of the PtN7N-doped (a) CBP and (b) BN-DBC-Ph$_2$ film.

Figure S2 Molecular orientation of the PtN7N-doped BN-DBC-Ph$_2$ and CBP film.

Device configuration is as follows:

Glass substrate / ITO (100 nm) / Clevious HIL1.5 (30 nm) / α-NPD (30 nm) / host: 40 wt%PtN7N

Measurement and analysis conditions are as follows:

  Detection method: Total electron yield (TEY)

  Measurement angle: 90°, 54.7°, 30°

  Normalization: N − σ*

From Figure S2, for CBP and BN-DBC-Ph$_2$ hosts, the N-absorption edge intensity of PtN7N exhibited only a small angular dependency; thus, PtN7N in CBP and BN-DBC-Ph$_2$ hosts exhibit marginal difference for molecular orientation.

Difference of operational stability between PtN7N and Ir(mppy)₃;

Figure S3 shows the device configuration and emitting-material-dependent operational stability. Using BN-DBC-Ph$_2$ as the host material, PtN7N exhibited almost same operational stability as that of Ir(mppy)$_3$.
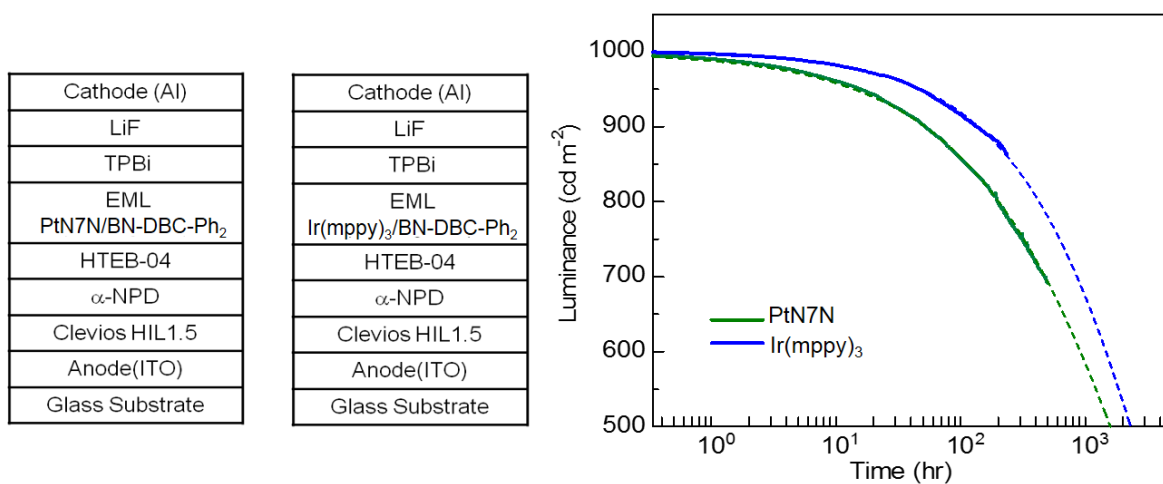
Cathode (Al)
LiF
TPBi
EML PtN7N/BN-DBC-Ph$_2$
HTEB-04
α-NPD
Clevios HIL1.5
Anode(ITO)
Glass Substrate

Cathode (Al)
LiF
TPBi
EML Ir(mppy)$_3$/BN-DBC-Ph$_2$
HTEB-04
α-NPD
Clevios HIL1.5
Anode(ITO)
Glass Substrate

Figure S3 Device configuration and emitting-material-dependent operational stability.

Optical design of the TE-PHOLED (simulation results);

To optimize the optical length of the micro-cavity and capping layer, the thickness of PEDOT: PSS and TPBi capping layers were calculated.
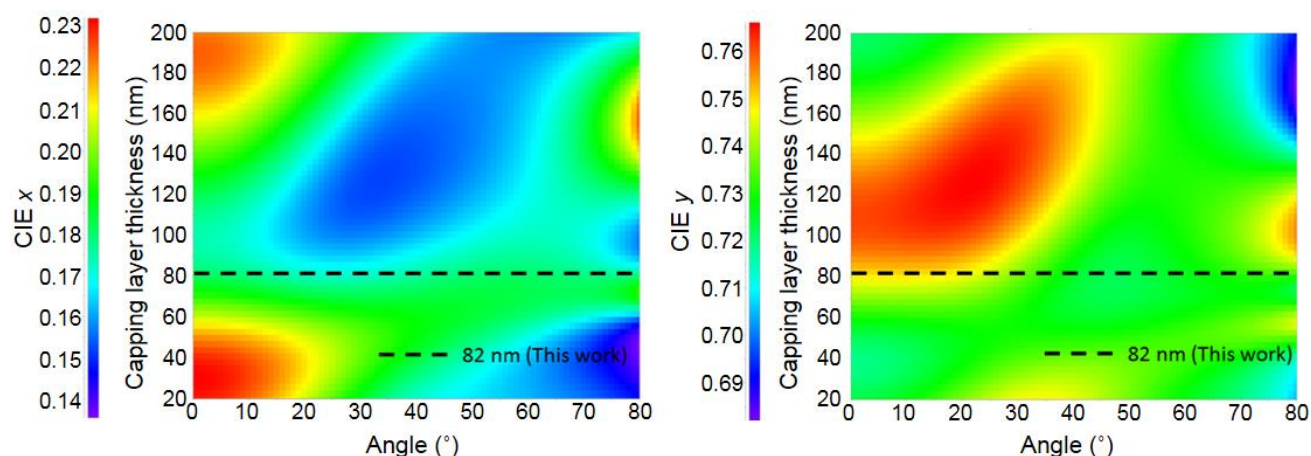
(a)
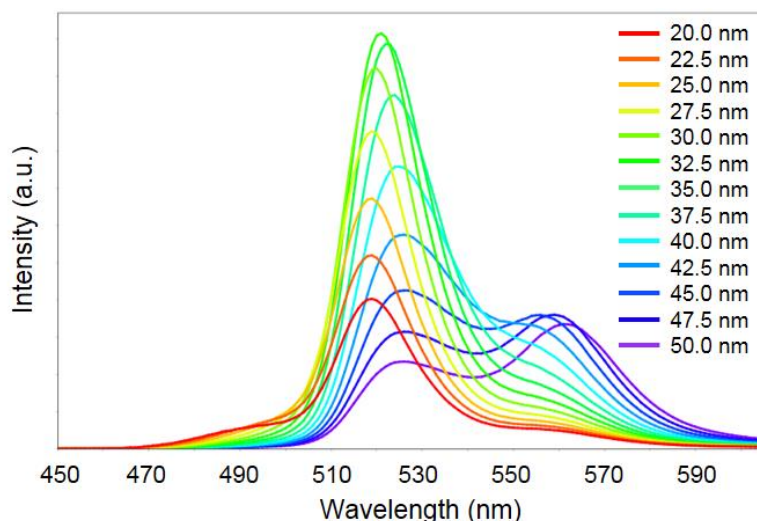
(b)

Figure S4 (a) EL emission of TE-PHOLED with a PEDOT: PSS thickness of 20–50 nm. (b) Capping-layer-thickness-dependent CIE x-y color coordinate at viewing angles of 0° to 80°.

Although the change of the CIE x-y color coordinate according to the viewing angle is the most stable for a capping layer film thickness of ~70 nm, the color purity at the front of the device is not sufficient (Figure 4(b)). On the other hand, although the chromaticity at the front of the device is the best for a capping layer film thickness of ~110 nm, the change in chromaticity coordinates caused by the angle change also proportionally increased. To suppress the angle change of chromaticity while simultaneously increasing the chromaticity at the front of the device, an 82-nm-thick capping layer was used herein.
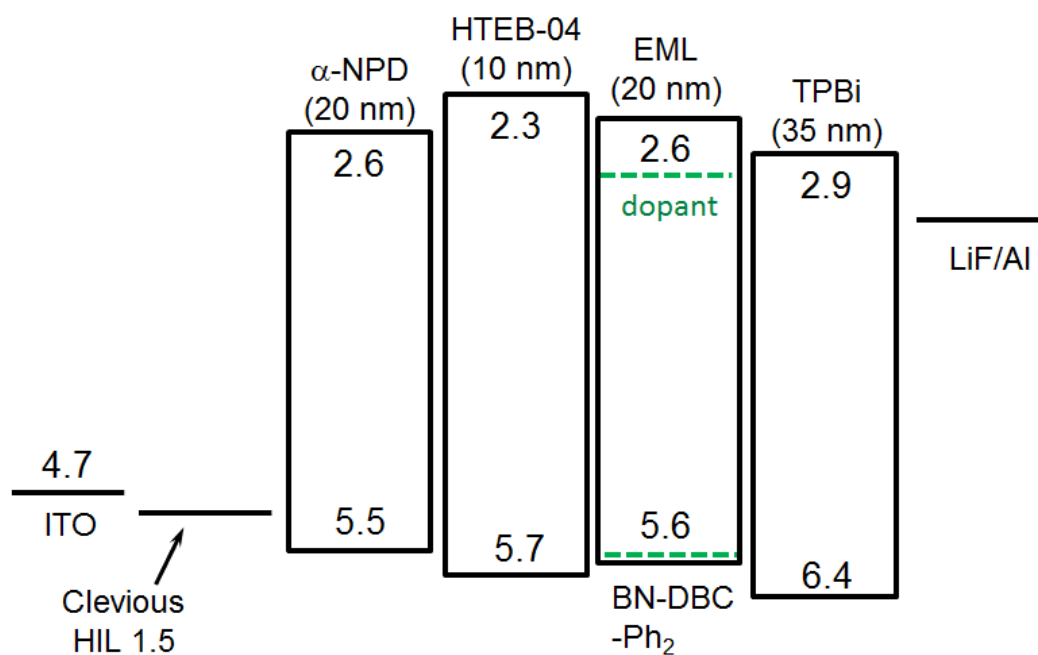
Energy level diagram of BE-PHOLEDs;

Figure S5 Energy level diagram of BE-PHOLED. The HOMO level was estimated from spectroscopic measurements of photoemission in air (AC-3, Rikenkeiki). The LUMO level was estimated by subtracting the optical band gap (Eg) from the HOMO level. The optical band gap was estimated using the cut-off wavelength of the absorption peak.

The color shift of TE-PHOLED with applied voltage;

The CIE *x-y* color coordinate of the TE-PHOLED changes slightly with the applied voltage since the electron-hole recombination zone shifts with the applied voltage. As applied voltage changing from 3 to 6 V, the CIE *x-y* color coordinate changes from (0.189, 0.740) to (0.183, 0.745).

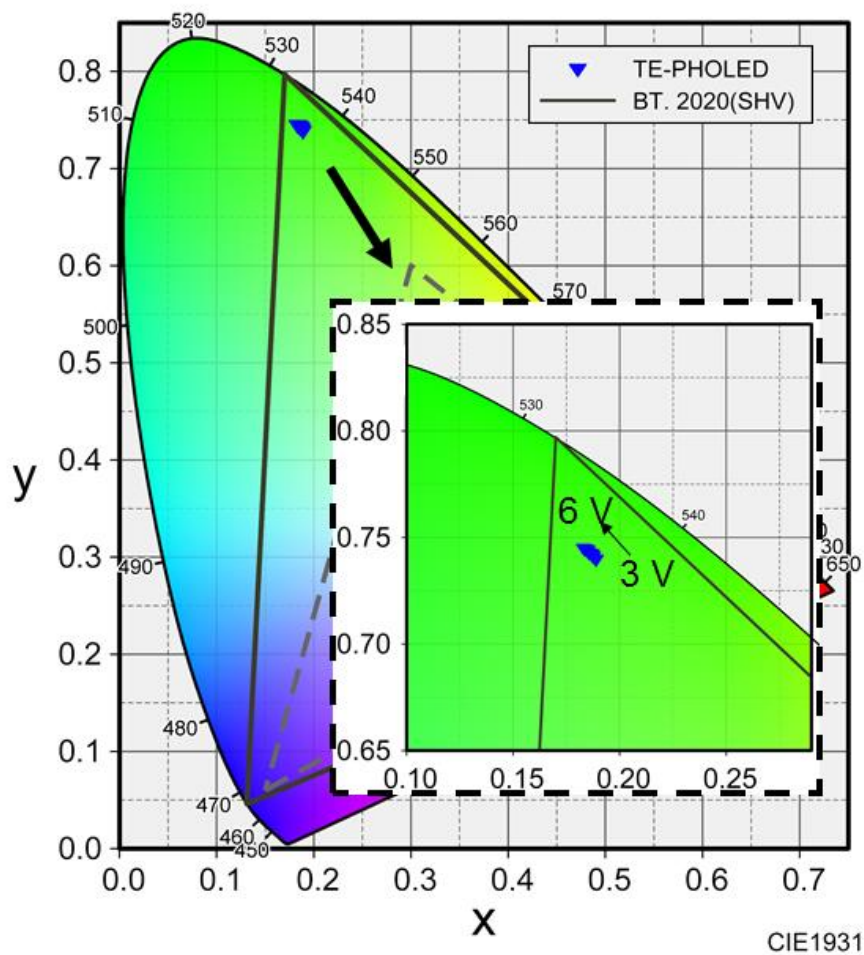**Figure S6** The CIE *x-y* color coordinates of the TE-PHOLED in different applied voltage.